Grain Size Effects on the Mechanical Behavior of Open-cell Nickel Foams**

By *V. Goussery,* Y. Bienvenu, S. Forest, A.-F. Gourgues, C. Colin, J.-D. Bartout*

The dependence of the mechanical behavior of nickel foams upon their grain size was studied. A metallurgical characterization of the grain growth during heat treatment was performed. The grain size effects on the mechanical properties was then studied, namely, via the Hall-Petch law. The present results obtained with foams were compared with literature data on bulk pure nickel and with nickel foils of 10 and 50 μm in thickness which are good candidates for the modeling of the cell walls. The EBSD technique allowed observing the absence of preferred crystallographic orientations for both foams and foils. A mechanical model in the spirit of that by Gibson and Ashby was finally presented incorporating the grain size effect on yield strength and hardening modulus. This model provided a good estimation of the experimental data.

1. Introduction

Among many applications, nickel foams are dedicated to be used as an electrode element in Ni-MH batteries for hybrid vehicles. The first step in the nickel foam production at NiTECH is a nickel magnetron sputtering on a polyurethane foam. It results in a 0.1 μm thick nickel coating making the foam conductive for the next processing stage, i.e. an electrolytic deposition of up to 10 μm of nickel. Afterwards, a heat treatment is then performed: the polyurethane foam is first removed from the structure by a non-isothermal combustion under air up to 600 °C, then the foam is annealed at about 1000 °C in a reducing atmosphere to meet the targets for elongation and strength to fracture.

To optimize the final anneal, nine heat treatment conditions were investigated in order to understand the grain growth mechanisms in nickel foams, and to evidence the grain growth effects on mechanical properties such as yield strength (via the Hall-Petch law) and hardening modulus. A first comparison was made with literature results on bulk nickel. It is observed in literature that the dimensional parameters, like the thickness, may have an effect on the strengthening of metals.[1] For this reason, experimental results for nickel foams were also compared with data obtained on thin materials, namely foils of 10 μm and 50 μm in thickness, which present a high surface-to-volume ratio like nickel foam struts. The 10 μm thick foil has a thickness close to that of the strut wall and the 50 μm thick foil made it possible to observe the thickness effect.

2. Experimental Procedures

2.1. Materials

Nickel foams were provided by NiTECH. The chemical purity is at least 99.9 %. The weight per unit area is 500 g/m^2, with a thickness of 1.6 mm, thus the relative density ρ^*/ρ is 0.035. The number of pores per inch (PPI) is 110, corresponding to an average cell size of 500 μm (Fig. 1a). The open-cell foam consists of hollow struts (Fig. 1b). The wall thickness varies through the foam thickness from 8 (in the mid-thickness of the foam) to 11 μm (near the foam surface). The grain structure, in the as-received state, is a "bamboo" microstructure, i.e. one columnar grain in the thickness of the strut walls (Fig. 2). Besides, the cell geometry is anisotropic. Previous

[*] ■*Please check title and addresses of authors!*■
Dr. V. Goussery, Dr. Y. Bienvenu, Dr. S. Forest,
Dr. A.-F. Gourgues, Dr. C. Colin, Dr. J.-D. Bartout
Centre des Matériaux Pierre-Marie Fourt
UMR CNRS 7633
Ecole Nationale Supérieure des Mines de Paris
BP 87, 91003 Evry Cedex, France
E-mail:

[**] *The authors gratefully acknowledge Dr Michel Croset and the industrial partners NiTECH and INCO. This work was supported by the CEE under contract PROBATT ENK6-CT2000-00102.*

 DOI: 10.1002/adem.200405153

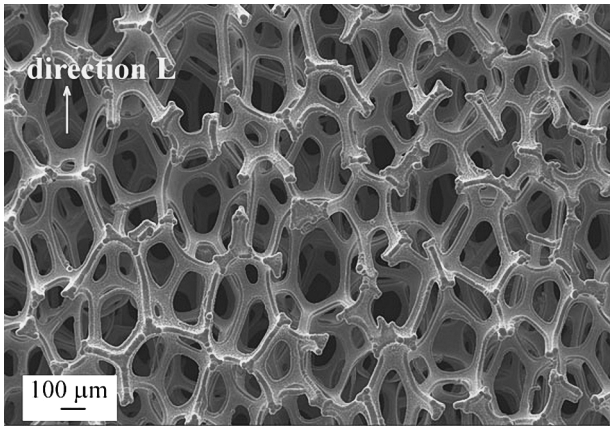

(a)

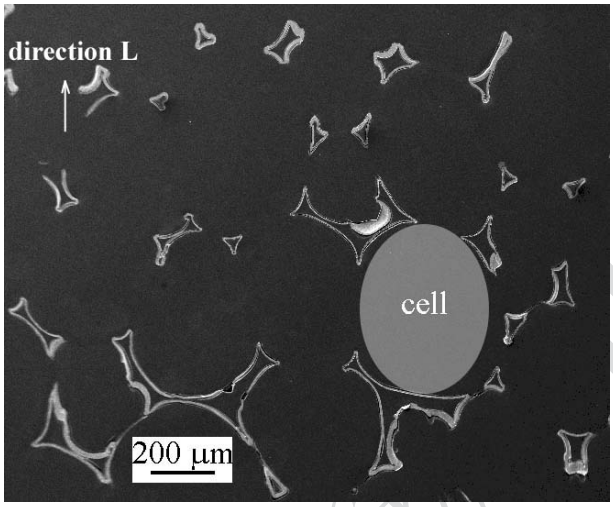

(b)

Fig. 1. Scanning Electron Microscope (SEM) micrographs of nickel foams. a) global view. (b) polished cross-section.

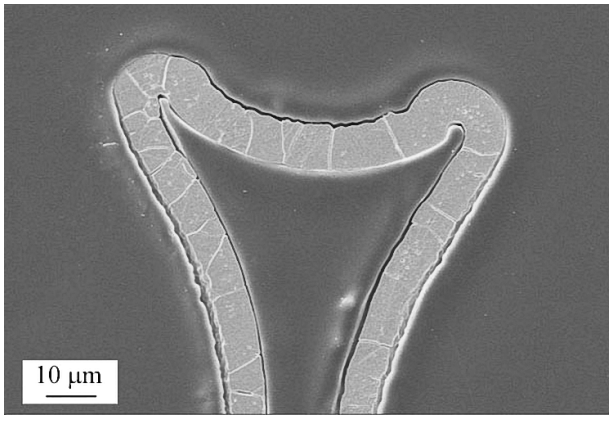

Fig. 2. SEM micrograph of an etched cross-section of a nickel strut: "bamboo" microstructure.

studies[2,3] revealed that the anisotropic character was caused by the structure of the polyurethane foam and also by elongation during the manufacturing. Thus, two directions are considered, direction L (direction of the foam movement during the process) and direction T (perpendicular to direction L).

The considered nickel foils from Goodfellow are 10 μm and 50 μm in thickness, with a chemical composition of respectively 99.95 % and 99.98 % of nickel. The annealed 50 μm thick foil has a grain size of 57 μm. The 10 μm thick foil had been annealed and exhibits a grain size of about 7 μm.

2.2. Heat Treatments

After the polyurethane combustion step, foams were isothermally heat treated at temperatures ranging from 850 °C to 1050 °C during times from 30 sec to 8 min, and foils from 400 °C to 1300 °C during times from 3 to 6 h. Then, they were slowly cooled to room temperature. The furnace atmosphere was a N_2 / 10 % H_2 mixture to avoid oxidation of nickel and to be close to the current NiTECH processing conditions, where a reducing atmosphere is used to eliminate all traces of carbon which could make the foam brittle.

2.3. Metallurgical and Mechanical Characterization

Microstructural characterization was performed using a LEO VP1450 conventional scanning electron microscope (SEM) and a high resolution LEO DSM 982 Gemini field emission gun SEM. Grain boundaries were observed by backscattered electron imaging without any chemical etching or by secondary electron imaging after an acetic acid/nitric acid etching.

The EBSD (Electron Back Scatter Diffraction) technique was used in the high resolution SEM to study the texture of the nickel struts in a foam and that of the annealed foils. The EBSD technique allowed the determination of the local crystallographic orientation by indexing pseudo-Kikuchi patterns.[4] Furthermore, this technique made the grain size measurements easier by eliminating the annealing twins from the grain distributions. The high voltage used in the SEM was 20 keV, the working distance 19 mm and the sample was tilted by 70°. The foams were mounted in resin and mechanically polished with diamond paste down to 1 μm and then with a colloidal silica suspension. The foils were polished with diamond paste down to 1 μm and then, electropolished in a solution containing 45 % butoxyethanol, 45 % acetic acid, and 10 % perchloric acid at room temperature under 12 to 16 V.

The room temperature tensile properties were determined by uniaxial tests along direction L with a gauge length of 70 mm for foams and 22 mm for foils, at room temperature and with a 500N load cell. The nickel foam samples, with a section of 25*1.6 mm^2, were 150 mm in length. With this configuration, about 2 or 3 cells were found through the specimen thickness, and 50 in the width. The nickel foil samples were 10 mm in width and 150 mm in length.

ADVANCED ENGINEERING MATERIALS

3. Experimental Results and Discussion

3.1. Grain Growth Mechanisms

Due to its medium stacking fault energy (128 $mJ.m^{-2}$)[5] nickel is prone to the formation of annealing twins ($\Sigma\perp\perp3$)[6,7] in foams as well as in foils. EBSD measurements (Fig. 3) demonstrate the increase in twin frequency with an increasing annealing temperature.

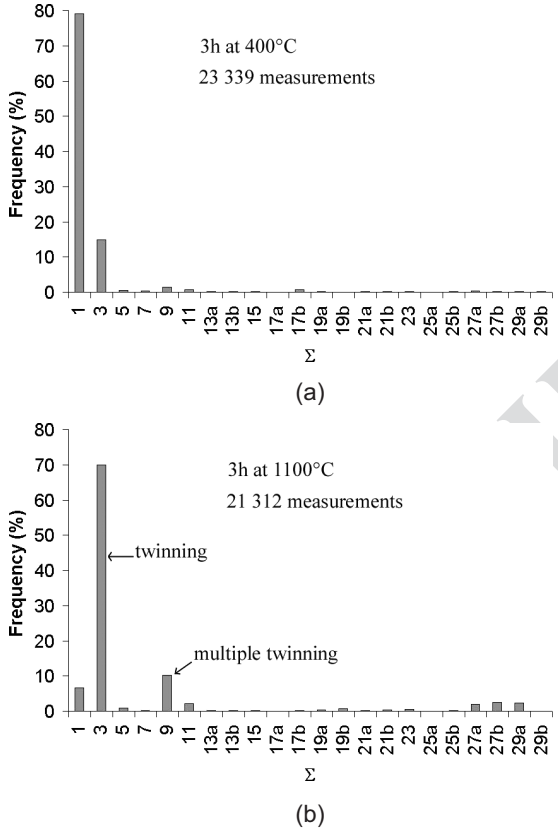

Fig. 3. Frequency of CSL (Coincidence Site Lattice) boundaries in nickel foils annealed for 3 h. a) at 400°C. b) at 1100 °C.

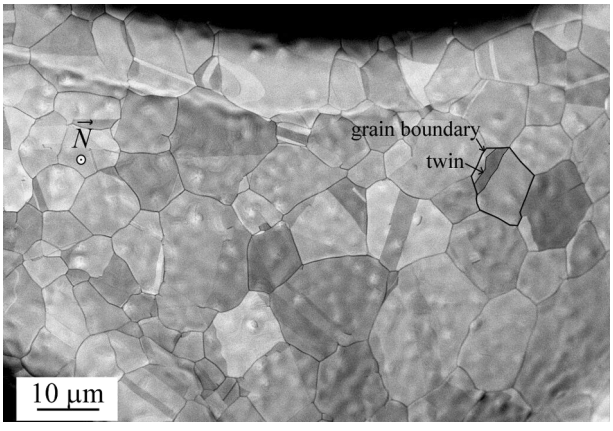

Fig. 4. Backscattered electron SEM micrograph of the surface of a nickel foam strut heat treated at 1050 °C for 8 min.

Concerning nickel foams, grain boundaries were easily observed on the strut surface due to the formation of thermal grooves whereas twin boundaries are not thermally grooved (Fig. 4). The roughness is inherent in the electrolytic deposition step. The grain size was measured in the plane perpendicular to the local normal of the strut ***N*** (Figs. 4 and 5b), and determined by conventional image analysis techniques. The grain size distributions were rather broad and the mean grain size, d, was in the range from 5 to 12 µm. Consequently, two configurations were found: a few grains through the thickness (Fig. 5a) or a "bamboo" microstructure (Fig. 5b).

In the 10 µm thick foil, the grain size measured on the side surface, ranged from 7 to 31 µm, that is to say, up to three times the foil thickness (Fig. 6a). As for foams, two configura-

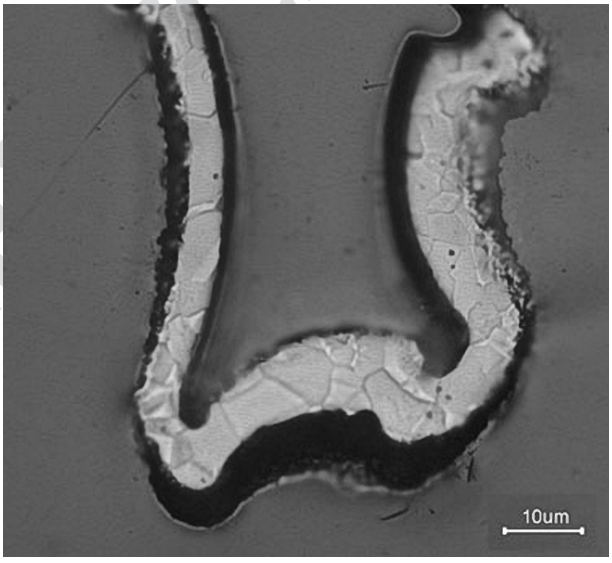

(a)

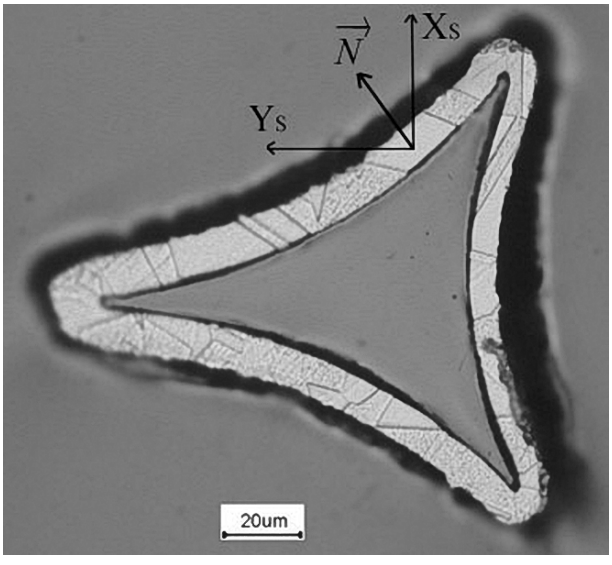

(b)

Fig. 5. Optical micrographs of a section of nickel foams after chemical etching and a heat treatment. a) at 850 °C for 2 min. (d = 6 µm). b) at 1050 °C for 8 min. (d = 12 µm).

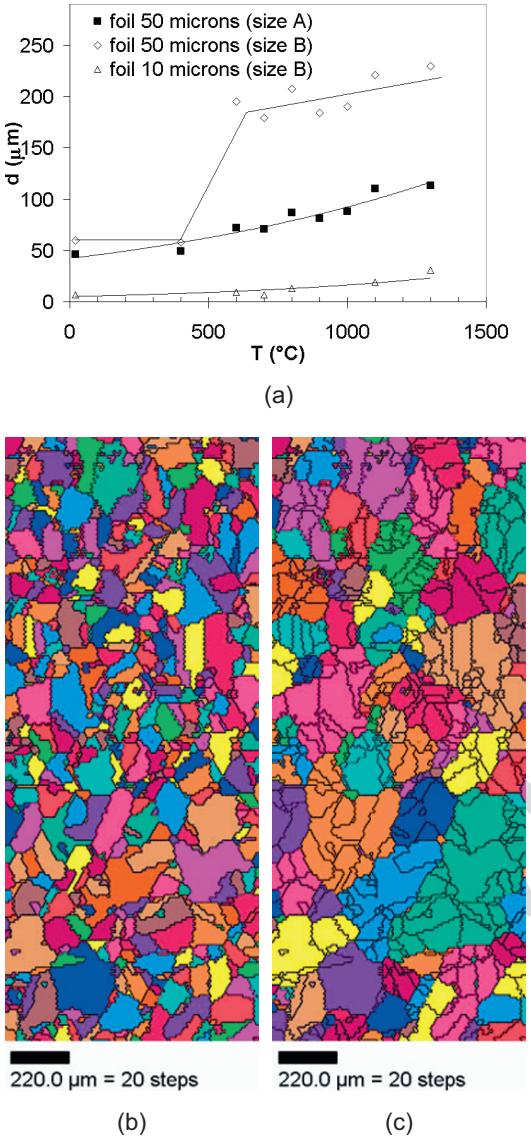

Fig. 6. Effect of twinning on the grain size. a) mean grain size in nickel foils after heat treatments for 3 h. b) EBSD grain map (one color per grain) after 3 h at 1100 °C with the black lines indicating misorientations higher than 15°. c) EBSD grain map of the same area after having eliminated twin boundaries (60° <111>)

tions were possible, for small grain size, the thickness was polycrystalline and once d reached 10 μm, the microstructure was "bamboo". In the 50 μm thick foil, grain boundaries were not readily observed and the presence of numerous twins led to an inaccuracy in the grain size measurements. In this case, the EBSD technique was used for the grain size determination. The mean grain size was determined using two assumptions, by considering that twin boundaries were (filled symbols), or were not (open symbols) "true" grain boundaries. For the first assumption, grain size was called size A and in the second case it was denoted as size B (Fig. 6). To eliminate twin boundaries (60° <111>), the Brandon criterion was used (θmax ≈ 9°) and was found to be efficient. As a matter of fact, by using a more severe criterion, that is, a lower value of Σmax, the same map was obtained. When the measurements were made by keeping twins as parts of the grains (size B), the grain size attained rapidly 200 μm for heat treatments between 400 and 600 °C. Currently, no explanation is available for this rapid grain growth. Then, grain growth finally stagnated and the highest measured grain size was 240 μm, i.e. about five times the foil thickness. Furthermore the microstructure was always "bamboo".

Basically, normal grain growth usually stagnates once the grain size is comparable to the foil thickness.[1,8] This phenomenon is known as the specimen thickness effect.[9] Normal grain growth saturates (slows down and stops) once a "bamboo" microstructure develops, that is to say, once all grain boundaries intersect both side surfaces of the foil. While the driving force for grain growth in a sheet or film with a columnar structure is reduced compared to that in a bulk system, it does not vanish. To explain the termination of normal grain coarsening in foils, it is necessary to invoke the development of a drag force. For instance, Mullins[8] has proposed that the development of thermal grooves where grain boundaries intersect the surfaces of a foil could be responsible for the stagnation of normal grain growth by pinning the grain boundaries. This results in a limiting grain size of 2 to 3 times the foil thickness. If subsequent grain growth is observed, it is usually abnormal. In this case, a small fraction of the grain population continues to grow much faster than the majority of the grains. A similar phenomenon of abnormal grain growth has also been observed in metallic sheets, for example in pure Au,[10] Zn,[11] and Pt.[12] The promotion of abnormal grain growth may be caused by surface effects or by the presence of texture. For this reason, the texture of all three materials was analyzed.

3.2. Texture

The EBSD analysis was carried out for foils by performing classically automatic maps. In literature, the texture of annealed fcc thin films is found to have three components for the normal to the foils, i.e. <111>, <100> and random.[13,14] In our case, both 10 and 50 μm thick foils have no significant texture as seen in Figures 7 and 8.

Concerning foams, the presence of resin did not allow the realization of automatic maps, therefore the measurements were manually performed on strut sections (Fig. 9a). For each measurement, the certainty that the sample section was actually normal to lateral faces was obtained by checking that lateral faces were not visible. Only the local texture was considered, i.e. the crystallographic indices were calculated for the local normal to the strut walls in the plane (Xs, Ys), as indicated by the N direction in Fig. 9a. No preferred orientation of this normal with respect to the crystal frame could be evidenced (Fig. 9b). So, the nickel strut grains did not keep the texture inherent in the electrolytic deposition.

The texture is not clearly responsible for abnormal grain growth. To explain this phenomenon, grain growth might be

ADVANCED ENGINEERING MATERIALS

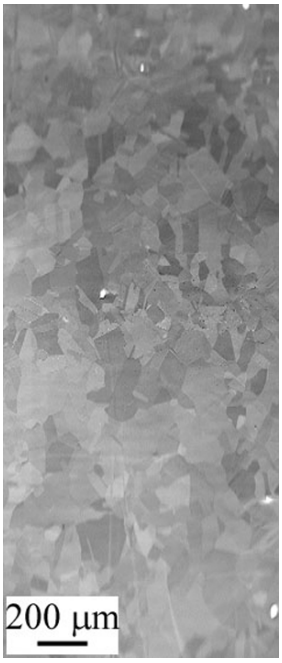

(a)

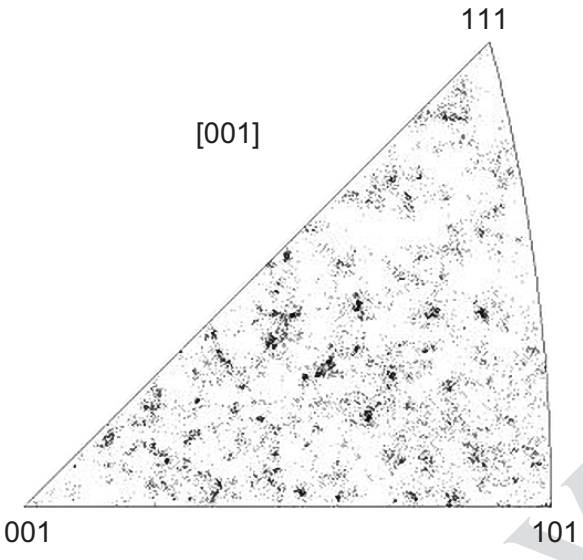

(b)

Fig. 7. 50 µm thick foil treated at 1100 °C for 3 h. a) electropolished sample. b) inverse pole figure showing the crystallographic orientation of the sample normal Zs.

(a)

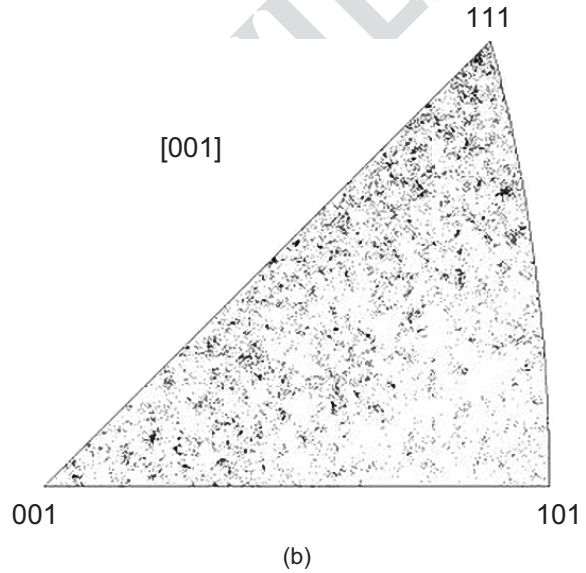

(b)

Fig. 8. 10 µm thick foil treated at 1100 °C for 3 h. a) electropolished sample. b) inverse pole figure showing the crystallographic orientation of of the sample normal Zs.

driven by the difference in surface energy between two adjacent grains.[5] Due to the high surface-to-volume ratio, grains exposed to surfaces are numerous and it is shown that only a few percent difference in surface energy enables abnormal grain growth. Most of the biggest grains are (111) oriented, i.e. according to the plane of minimal surface energy, nevertheless this trend is not sharp.

3.3. Grain Growth Activation Energy

The activation energy, E_a, associated with grain growth, was calculated for each material with the relationship:

$$d - d_0 = k \cdot t^{1/n}, \text{ with } k = k_0 \cdot \exp\left(\frac{-E_a}{RT}\right), \quad (1)$$

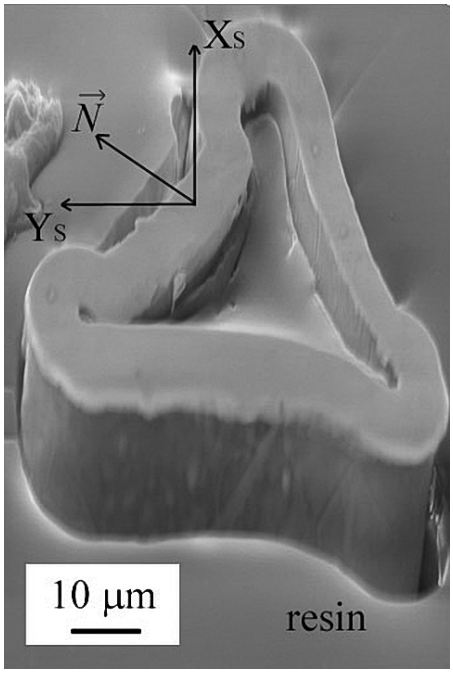

(a)

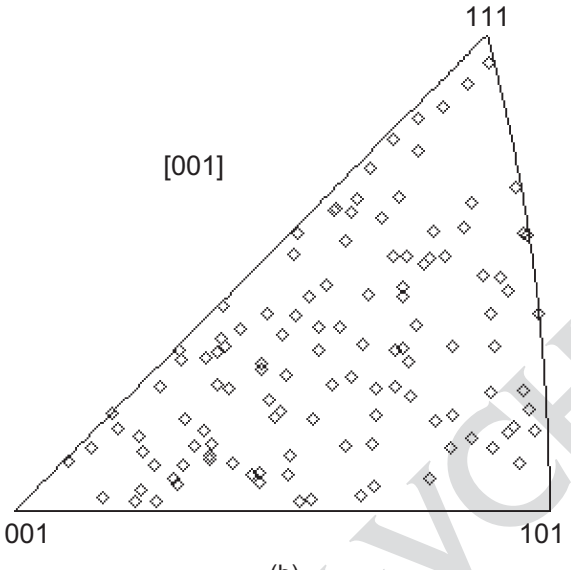

(b)

Fig. 9. a) Typical foam strut section used for EBSD measurements, the plane (Xs, Ys) belongs to the plane section. b) inverse pole figure of the local normal to the strut walls (120 point measurements).

Table 1. Activation energies associated to grain growth for foils and foams

	Nickel foils (10 μm) $7 < d < 31$ μm	Nickel foils (50 μm) $57 < d < 195$ μm	Nickel foams $5 < d < 12$ μm
T (°C)	400 – 1300	400 – 600	850 – 1050
t (min)	180	180	0.5 – 2 – 8
d_0 (μm)	7	57	5
E_a (kJ/mol.)	98	120	116 (average for the 3 times)

where d is the grain size B, d_0 the initial grain size, t the annealing time, n the exponent of grain growth, k_0 a constant, R the gas constant, and T the annealing temperature. The values are listed in Table 1 and are close to the value for boundary self-diffusion in pure nickel (115 kJ/mol)[15] and to that found for grain growth of bulk nanocrystalline nickel (102 kJ/mol).[16]

3.4. Mechanical Tensile Properties

An increase in yield strength with decreasing grain size is characteristic of many metals and alloys and is known as the Hall-Petch effect as long as the dependence on grain size d follows an inverse square root relationship: $\sigma_y = \sigma_0 + \kappa_y.(d)^{-1/2}$, where σ_y is the yield strength in MPa, and d is in mm. The parameters σ_0 and κ_y (in MPa.mm$^{1/2}$) are material constants. In literature, numerous relations are found for bulk pure nickel, e.g., $\sigma_y = 18.29 + 6.32d^{-1/2}$[17], $\sigma_y = 21.80 + 4.97d^{-1/2}$[18], $\sigma_y = 14.14 + 10.18d^{-1/2}$[19].

Foils and foams (Fig. 10) follow a Hall-Petch law as long as the grain size is smaller than the strut wall or foil thickness. Vertical arrows indicate the changes in slope, located at 15 μm for the 10 μm thick foil, and at 8 μm for foams. For higher values of grain size, a saturation in yield strength was observed, the points in the box in Figure 10 oscillate only between 22 and 33 MPa with a mean slope κ of 0.5 MPa.mm$^{1/2}$. It can be explained by the fact that yielding is induced by motion of dislocations which are constrained to "channel" through the foil.[1] For our materials, once grain size reaches the metal thickness, as there is no oxide layer, the foil surface is penetrable to dislocations, and dislocation loops can easily escape across free surfaces. This assumption is confirmed by the presence of numerous slip lines after fracture of both foams and foils (Fig. 11).

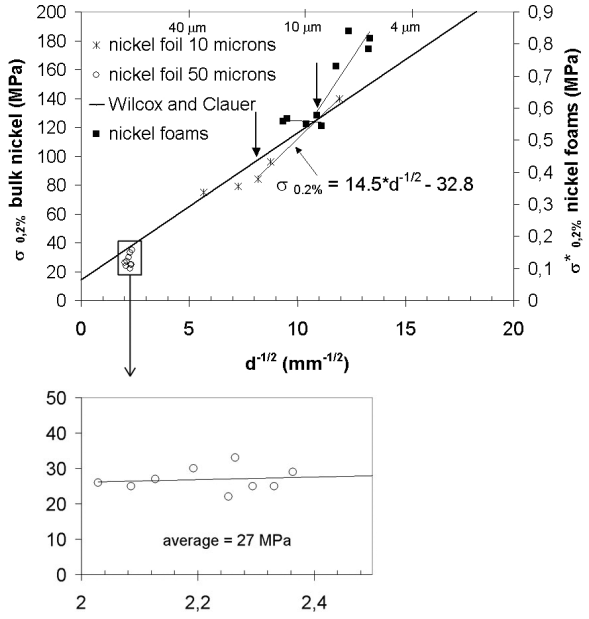

Fig. 10. Hall-Petch law for foils and foams compared with literature data on bulk nickel.

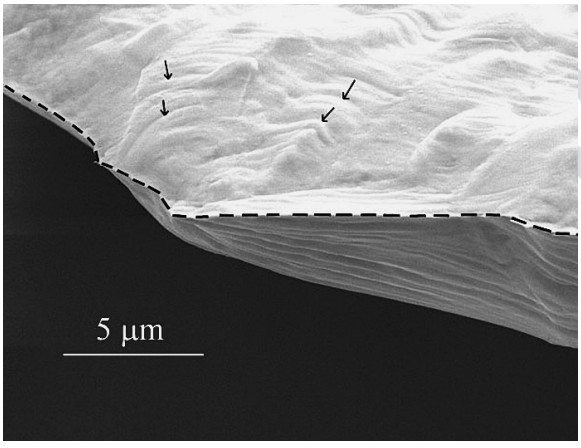

(a)

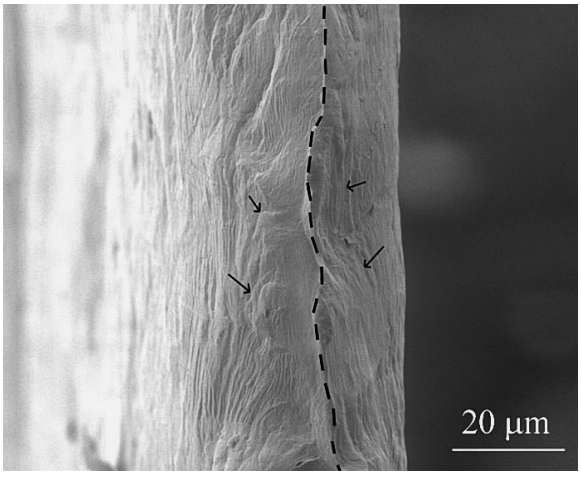

(b)

Fig. 11. SEM micrographs of fractured. a) nickel foam. b) 50 µm thick nickel foil. Some slip lines are indicated with arrows and the dashed lines indicate the fracture line (100 % reduction in thickness)

The constitutive response of both nickel foams and foils is correctly described by linear hardening (Fig. 12). Concerning the hardening modulus H of foils, two populations of points were noted according the thickness foil (Fig. 13a). The value of H remained rather constant for the 50 µm thick foil (1700 MPa on average), whereas it decreased from 2500 to 1450 MPa for the 10 µm thick foil. Concerning nickel foams, H^* decreased from 13 to 9 MPa with an increasing grain size (Fig. 13b).

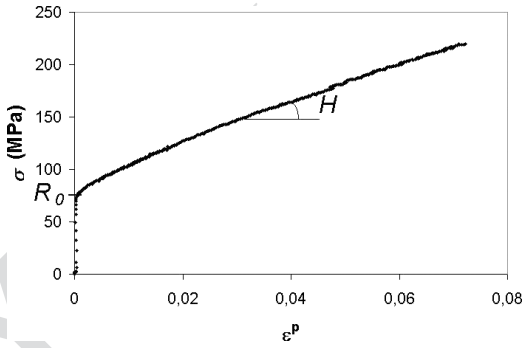

Fig. 12. Tensile test for the 10 µm thick foil treated 6 h at 900 °C, ε_p is the plastic strain, R_0 the yield strength and H the hardening modulus.

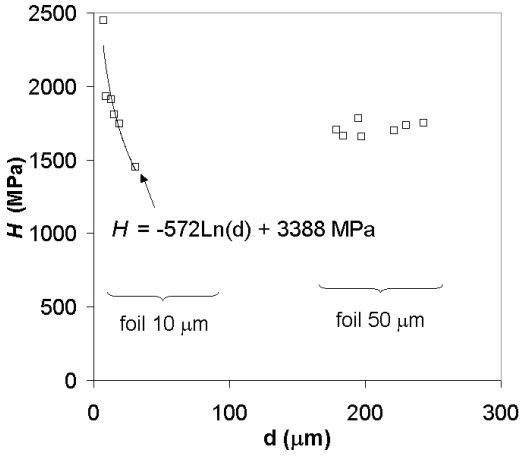

(a)

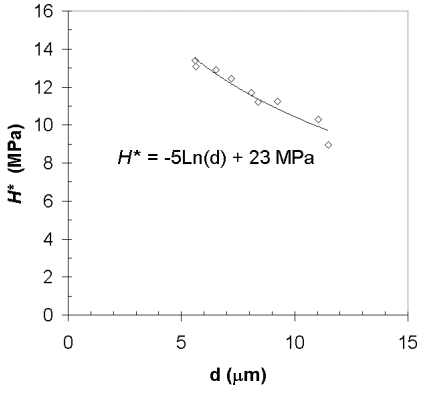

(b)

Fig. 13. Hardening modulus as a function of grain size for a) nickel foils b) nickel foams.

4.1. Modeling

Experimental tensile properties were modeled following an approach inspired by Gibson and Ashby[20], extended to the elastic-plastic case. The mechanical properties of cellular solids are directly related to those of the cell wall metal and the foam geometry. This micromechanical model is based on the assumption that the main deformation mode is bending of the struts. Two mechanical properties were considered, the proof stress $\sigma_{0.2\,\%}$ and the hardening modulus H. The established relationships are:

$$\sigma^*_{0.2\%} = \alpha_1 \cdot \frac{1}{2} \cdot \left(\frac{\rho^*}{\rho}\right)^{\frac{3}{2}} \sigma_{0,2\%} \quad (2)$$

$$H^* = \alpha_2 \cdot \frac{2}{3} \cdot \left(\frac{\rho^*}{\rho}\right)^{2} H \quad (3)$$

where $\sigma^*_{0.2\,\%}$ is the proof stress of the foam, ρ^* its density, and H^* its hardening modulus. Constants α_1 and α_2 are dimensionless geometrical parameters. Values without superscript are those of bulk nickel. The 10 μm thick foil has a thickness close to that of strut walls and is consequently a good candidate to model the nickel behavior taking into account the thickness effect. Thus, the model was applied with the Hall-Petch law ($\sigma_{0.2\,\%} = -32.8 + 14.5d^{-1/2}$) and the relationship for H ($H = -572\ln(d) + 3388$) obtained for the 10 μm thick foil. These relationships between plastic properties of nickel foils and grain size were inserted to the foam model equations (1 and 2) and thanks to experimental data for nickel foams, parameters α_1 and α_2 could be fitted. The value of α_1 was 1.5 and α_2 was estimated to 6.3. Finally, the model enabled to predict the proof stress with an accuracy of 8 %, and 4.5 % for the hardening modulus, for grain sizes ranging from 5 to 12 μm. The model gave a good estimation of the foam behavior (Fig. 14) and also provided correct results for another foam with a relative density of 0.029[21].

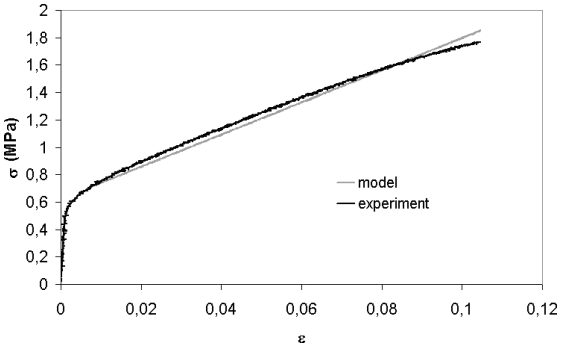

Fig. 14. Experimental tensile test and tensile behavior predicted by the model for a grain size of 11 μm.

5. Conclusion

The experimental study of grain growth and its influence on the mechanical properties of nickel foils and open-cell foams gave the following results:

During the annealing treatment, the grain size reached three to four times the thickness of nickel foils. Thus, no pinning effect on boundaries due to thermal grooving was observed. This behavior departed from the results usually obtained with bulk pure nickel. On the contrary, for nickel foams, the maximal grain size (12 μm) was of the order of the strut wall thickness (10 μm). Nevertheless, we cannot exclude that a longer heat treatment could lead to a much higher grain size.

No preferred crystallographic orientation was noted for both foils and foams. Consequently, abnormal grain growth was probably due to the high surface-to-volume ratio of foils with respect to bulk specimen geometry.

The yield strength of non-oxidized samples decreased with increasing grain size up to the local metal thickness for both foams and foils. For higher grain size, the elastic-plastic properties appeared to be driven by escape of dislocation loops across free surfaces.

The proposed model gave a good estimation of the mechanical properties of foams from those of foils.

Received: March 23, 2004

[1] E. Arzt, *Acta Mater*. **1998** *46*, 5611.
[2] X. Badiche, S. Forest, T. Guibert, Y. Bienvenu, J.-D. Bartout, P. Ienny, M. Croset, H. Bernet, *Mater. Sci. Eng. A* **2000**, *289*, 276.
[3] T. Dillard, F. N'Guyen, S. Forest, Y. Bienvenu, J.-D. Bartout, L. Salvo, R. Dendievel, E. Maire, P. Cloetens, C. Lantuéjoul, *Proceedings Int. Conf. Cellular Solids and Metal Foaming Technology*, (eds : J. Banhart, N. A. Fleck, A. Mortensen), MIT Press-Verlag Germany **2003**, p. 301.
[4] V. Randle, *Microtexture determination and its applications*, The Institute of Materials, London **1992**, Chapters 1 and 2.
[5] F. J. Humphreys, M. Hatherly, *Recrystallization and Related Annealing Phenomena*, Pergamon, Oxford **1995**, Chapter 9.
[6] C. B. Thomson, V. Randle, *Scripta Mater*. **1996**, *35*, 385.
[7] C. B. Thomson, V. Randle, *J. Mater. Sci.* **1997**, *32*, 1909.
[8] W. W. Mullins, *Acta Metall*. **1958**, *6*, 414.
[9] C. V. Thompson, *Annu. Rev. Mat. Sci.* **1990**, *20*, 245.
[10] S. Mader, R. Feder, P. Chaudhari, *Thin Solid Films* **1972**, *14*, 63.
[11] W. A. Miller, W. M. Williams, *J. Inst. Met*. **1964**, *93*, 125.
[12] M. McLean, H. Mykura, *Acta Metall*. **1965**, *13*, 1291.
[13] C. V. Thompson, R. Carel, *Mater. Sci. Forum* **1996**, *204–206*, 83.
[14] J. Greiser, P. Müllner and E. Arzt, *Mater. Sci. Forum* **1998**, *273–275*, 237.

[15] H. J. Frost, M. F. Ashby, *Deformation mechanism maps: the plasticity and creep of metals and ceramics*, **1982**, Pergamon Press.
[16] M. C. Iordache, S. H. Whang, Z. Jiao, Z. M. Wang, *Nanostructured Materials* **1999**, *11*, 1343.
[17] K. C. Hsu quoted by A. Mortensen during a lecture on metallurgy in **2000**.
[18] A. W. Thompson, *Acta Metall*. **1975**, *23*, 1337.
[19] B. A. Wilcox, A. H. Clauer, *Acta Metall*. **1972**, *20*, 743.
[20] L. J. Gibson, M. F. Ashby, *Cellular solids: Structure and properties*, 2nd edition, Cambridge university press, Cambridge **1997**, Chapter 5.
[21] V. Goussery-Vafiadès, PhD thesis, Ecole Nationale Supérieure des Mines de Paris, Paris **2004**.